Selective Identification of Hedgehog Pathway Antagonists By Direct Analysis of Smoothened Translocation to the Primary Cilium

Yu Wang *et al.*

Supplementary Figures (18)

Supplementary Figure Legends:

Supplementary Fig.1 Differential modulation of Smo cilial translocation and its signaling by several antagonists. **(a)** A schematic showing different Smo ciliary translocation behaviors induced by different Hh antagonists. Although all inhibited Smo activity, SANT-1, SANT-2, and GDC0449 inhibited Smo ciliary accumulation, whereas the direct Smo antagonist Cyc and FKL, a PKA activator, that indirectly affects pathway activity, both promote Smo accumulation to the PC. **(b-c)** Treatment with Hh antagonists (Cyc: 5 μM; FKL: 100 μM ; SANT-1: 500nM; GDC0449: 500nM) modifies Smo cilial localization (b) and inhibit Shh-stimulated pathway activity (P<1E-4 in t test) (c). SAG was included as a control agonist that has been shown to bind Smo and promote ligand independent Smo accumulation on the PC. Data show the mean from quadruplicate treatments (± the standard deviation, S.D.).

Supplementary Fig.2. The workflow for a Smoothened cell-based screen monitoring accumulation at the primary cilium. Small molecule libraries were applied to Smo::EGFP/Ivs::tagRFPT cells. Potential antagonists of Smo cilial accumulation were identified in an assay based on movement of Smo::EGFP.

Supplementary Fig.3. Validation of high content Smo antagonist screen with SANT-1. **(a)** Representative images of the dose-dependent inhibition of Smo::EGFP cilial accumulation by SANT-1. The concentrations of SANT-1 used to obtain these images were 0, 1.5nM, 14nM, 123nM, 1111nM from left to right. Scale bar: 5μm. **(b)** Key

measurements from high content image analyses. The mean (±S.D) shown is based on four replicates.

Supplementary Fig.4 Plots of relative Smo::EGFP+ cilium count normalized upon Shh+DMSO treated samples for putative Smo antagonist screen. Each dot represents the measurement of over one thousand cells in each well. Compound libraries were assayed at 10μM for this plot. SANT-1 and SAG were used at 1μM and Cyc was used at 10μM.

Supplementary Fig.5 Indentification of AntagVIII. **(a)** structure. **(b-d)** AntagVIII inhibited both Smo cilial accumulation (b and c) and Hh pathway activity (d). Each treatment was analyzed in quadruplicate, measuring over 300 cells for each sample. AntagVIII was used at 1.875 μM for the representative image in (b). Scale bar: 5μm **(e)** high content analyses on AntagVIII's dose dependent inhibition of Smo localization on the PC.

Supplementary Fig.6 Identification of AY9944. **(a)** Structure. **(b-d)** AY9944 inhibited both Smo cilial accumulation (b and c) and the Hh pathway activity (d). Each treatment was analyzed in quadruplicate, measuring over 300 cells for each sample. AY9944 was used at 10 μM for the representative image in (b). Scale bar: 5μm **(e)** high content analyses on AY9944's dose dependent inhibition of Smo localization on the PC.

Supplementary Fig.7 Identification of Itraconazole (ICZ) and Ketoconazole (KCZ). **(a)** Structures. **(b-d)** ICZ and KCZ inhibited both Smo cilial accumulation (b and c) and Hh

pathway activity (d). Each treatment was analyzed in quadruplicate, measuring over 300 cells for each sample. ICZ and KCZ were used at 3.3μM and 10 μM for representative images (b). Scale bar: 10μm **(e)** high content analysis of the dose dependent inhibition of Smo accumulation in the PC on ICZ or KCZ treatment.

Supplementary Fig.8 High content analyses indicate specific inhibition of Smo cilial localization by DY131 and GSK4716. High content measurements are displayed for the cell count, Ivs::tagRFPT positive cilial count, cilial Ivs::tagRFPT intensity and Smo::EGFP intensity in the PC. Samples were analyzed in quadruplicate images comprising 50-100 transfected cells. Data are plotted as the mean (±S.D.).

Supplementary Fig.9 DY131 does not inhibit Wnt signaling activity. Wnt signaling activity was measured in a Top-flash reporter assay[1]. A gradient of DY131 was applied to the cells with (Fold plotted) or without Wnt3a ligand (Control% plotted) conditioned medium. Means (±S.D.) from quadruplicate treatments are shown.

Supplementary Fig.10 Several ERR/ER ligands including tamoxifen, 4-hydroxytamoxifen(4-OHT) , diethylstilbestrol, and hexestrol do not alter Smo cilial localization in presence or absence of Hh ligand. **(a)** Structures of ERR/ER ligands. **(b)** Mean (±S.D.) of relative Smo::EGFP positive cilium count after treating cells with various doses of ERR/ER ligands in the absence (Fold plotted) or presence (Control% plotted) of Hh ligand. Each treatment was analyzed in quadruplicate, examining over 600

cells per sample. **(c)** Representative images. All compounds were used at a concentration of 15μM. Scale bar: 5μm.

Supplementary Fig.11 Accumulation of SmoM2 in the PC is refractory to SANT-1 or GDC0449 inhibition. Representative images (a and c) and quantification (b and d) of the cilial intensity of Smo::EGFP and SmoM2::EGFP. SANT-1 and GDC0449 were used at 1.1μM for the representative images; quadruplicate samples were analyzed and data show the means (±S.D.) of the EGFP intensity, examining over 300 cells in each treatment. Scale bar: 5μm.

Supplementary Fig.12 SmoM2 mutation confers resistance to inhibition by Cyc, SANT-1, or GDC0449. Hh pathway activity was induced by Hh ligand, over-expressing Smo or SmoM2. Dose dependent inhibition of Hh/Smo/SmoM2 signaling by Cyc, SANT-1, or GDC0449 was measured in quadruplicate samples. Data show the mean (±S.D.).

Supplementary Fig13 DY131 inhibits SAG induced Smo cilial accumulation and signaling. Representative images (a) and image quantification (b) showing the mean (±S.D.) determined in quadruplicate samples, examining over 300 cells per sample. Scale bar: 5μm. Mean (±S.D.) of Gli luciferase activity measured in quadruplicated samples (c).

Supplementary Fig.14 High content analyses indicate specific inhibition of Smo cilial localization by SMANT and SMANT-2. High content measurements are displayed for

the cell count, Ivs::tagRFPT positive cilium count, cilial Ivs::tagRFPT intensity and Smo::EGFP intensity in the PC. Samples were analyzed in quadruplicate images comprising 50-100 transfected cells. Data are plotted as the mean (±S.D.).

Supplementary Fig.15 SMANT does not activate nor profoundly inhibit Wnt signaling activity. Wnt signaling activity was measured in a Top-flash reporter assay[1]. A gradient of SMANT was applied to the cells with (Fold plotted) or without Wnt3a ligand (Control% plotted) conditioned medium. Means (±S.D.) from quadruplicate treatments are shown.

Supplementary Fig16 SMANT does not inhibit Cyc induced Smo cilial accumulation, whereas DY131, SANT-1, and GDC0449 effectively compete with Cyc. **(a)** representative images of cells treated with 5 µM Cyc and DMSO, GDC0449 (7.5µM), SANT-1(7.5µM), DY131(7.5µM), or SMANT (15µM) respectively. **(b)** image quantification showing the mean (±S.D.) determined in quadruplicate samples, examining over 300 cells per sample. Scale bar: 5µm.

Supplementary Fig17 Examination of the effects of distinct Smo antagonists on Smo localization and Hh pathway activity. **(a)** Measurement of Hh signaling in Gli transcription reporter assays following treatment with either vehicle or Hh antagonists: Cyc (5µM), FKL (100µM), SANT-1 (500nM), and GDC0449 (500nM). Samples were analyzed in quadruplicate; mean is shown ±S.D. Pathway stimulation with Sonic hedgehog (Shh) was shorter (12 hrs) than in routine assays but a significant response was

observed in this short time frame (#p<0.04 and ##p<1E-4 in t test). * indicates statistically significant hyperactivity in a t test comparing pre-treated with vehicle treated cells (*p<0.02; **p<0.006 in t test). SANT-1 and GDC0449 pre-treated cells showed either a significant but lower induction (+p<0.05 in t test), or no reduction in activity (P>0.1 in t-test for the rest). **(b-e)** Representative images of Smo::EGFP in the PC (b and c) and quantified Smo::EGFP ciliary intensity (d and e); a slow turnover of Smo::EGFP was observed following Cyc (5μM) and FKL (100 μM) withdrawal. No measurable change was observed in Ivs::tagRFPT, an independent primary cilium marker, over the same time period. All the Ivs::tagRFPT images in this report were shifted leftwards by 5 pixels to clearly show both Smo::EGFP and Ivs::tagRFPT signals. Experiments were conducted in quadruplicate, analyzing over 300 cells in each sample. Fluorescent intensity was plotted as the mean (±S.D.). Scale bar: 5μm.

Supplementary Fig18 Cellular sensitivity to SAG stimulation after priming with various Hh antagonists. Hh signaling activity was measured in a Gli transcription reporter assay after pre-treatment with vehicle or various Hh antagonists including Cyc (5μM), FKL (100μM), SANT-1 (500nM), and GDC0449 (500nM). Samples were assayed in quadruplicate and means (±S.D.) were displayed. A short 12 hr stimulation with SAG induced a weak but significant response (#p<0.0002 in t test). * indicates statistical significant difference in t test when compared with cells treated with vehicle (*p<0.03; **p<0.005 in t test). In contrast, SANT-1 and GDC0449 treated cells showed a

significantly lower induction (+p<0.05 in t test) or no statistical difference (p>0.05 in t-test for remaining samples) when compared with cells treated with vehicle.

References

1. Corbit, K.C. et al. Kif3a constrains beta-catenin-dependent Wnt signalling through dual ciliary and non-ciliary mechanisms. *Nat Cell Biol* **10**, 70-6 (2008).

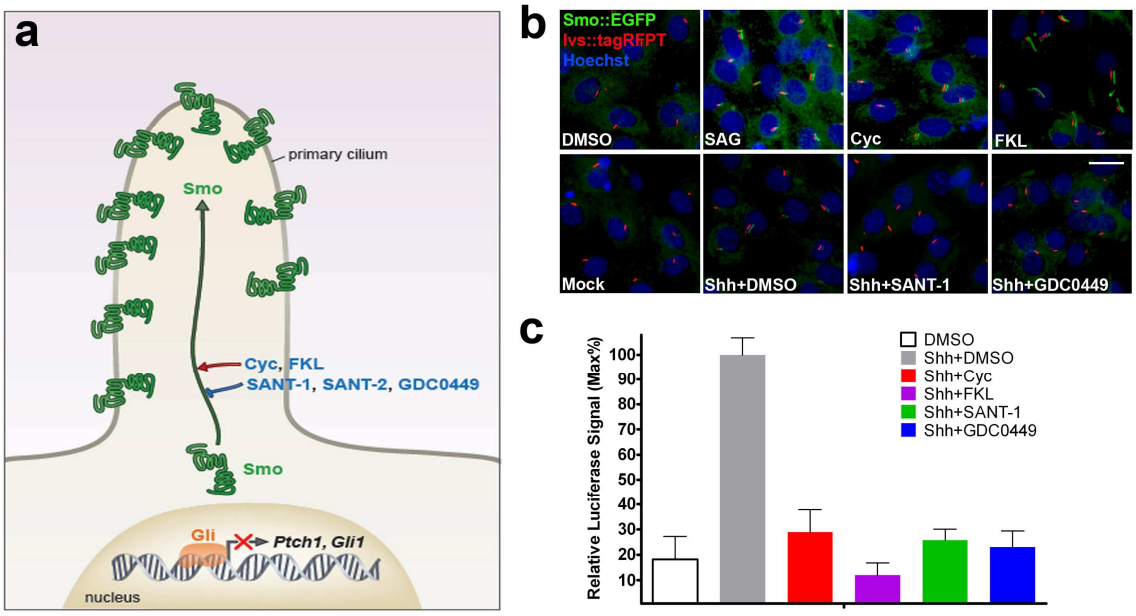

Supplementary Fig.1

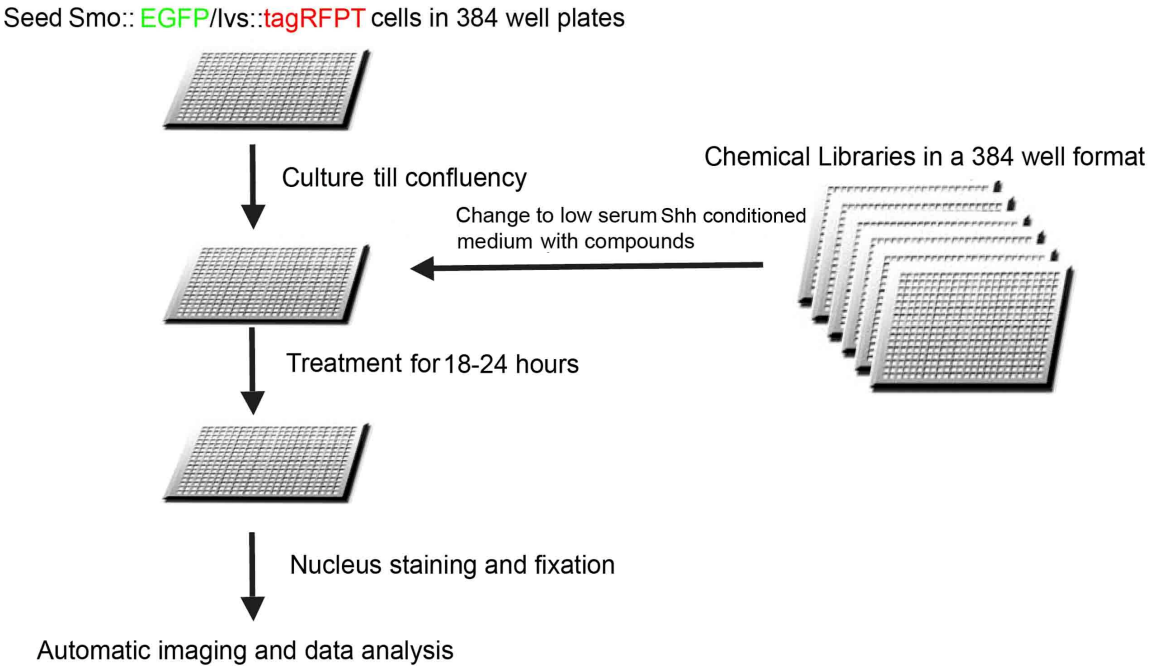

Supplementary Fig.2

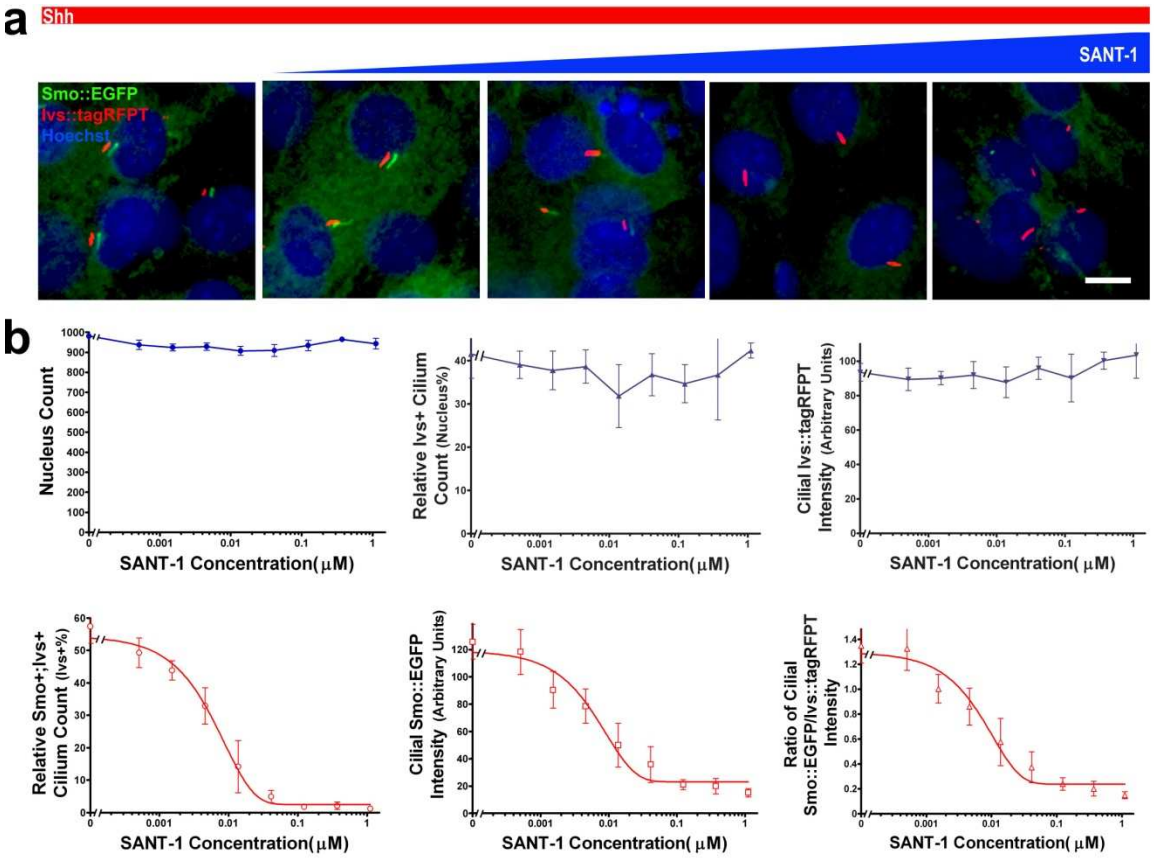

Supplementary Fig.3

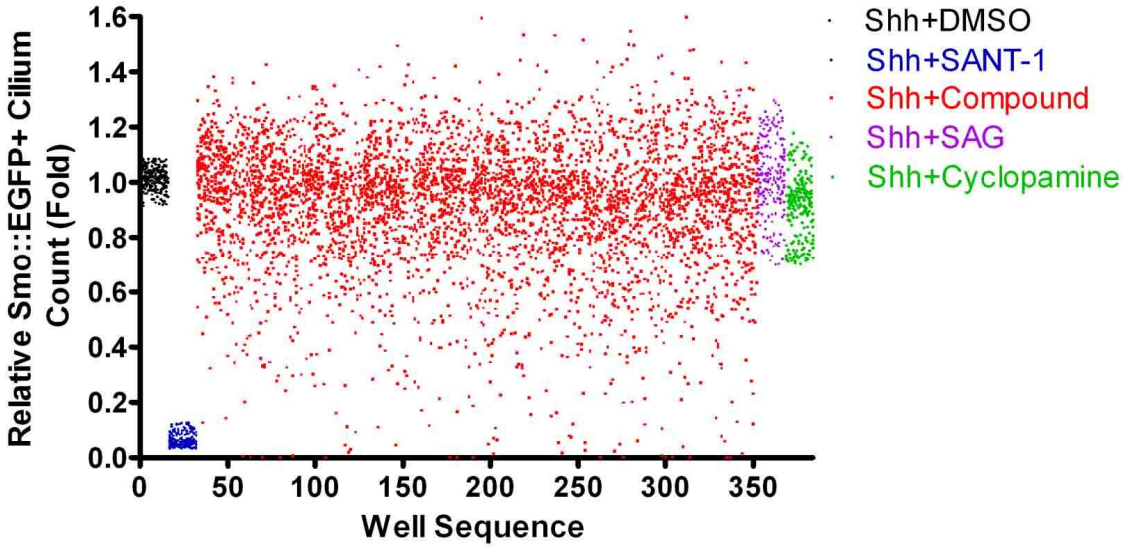

Supplementary Fig.4

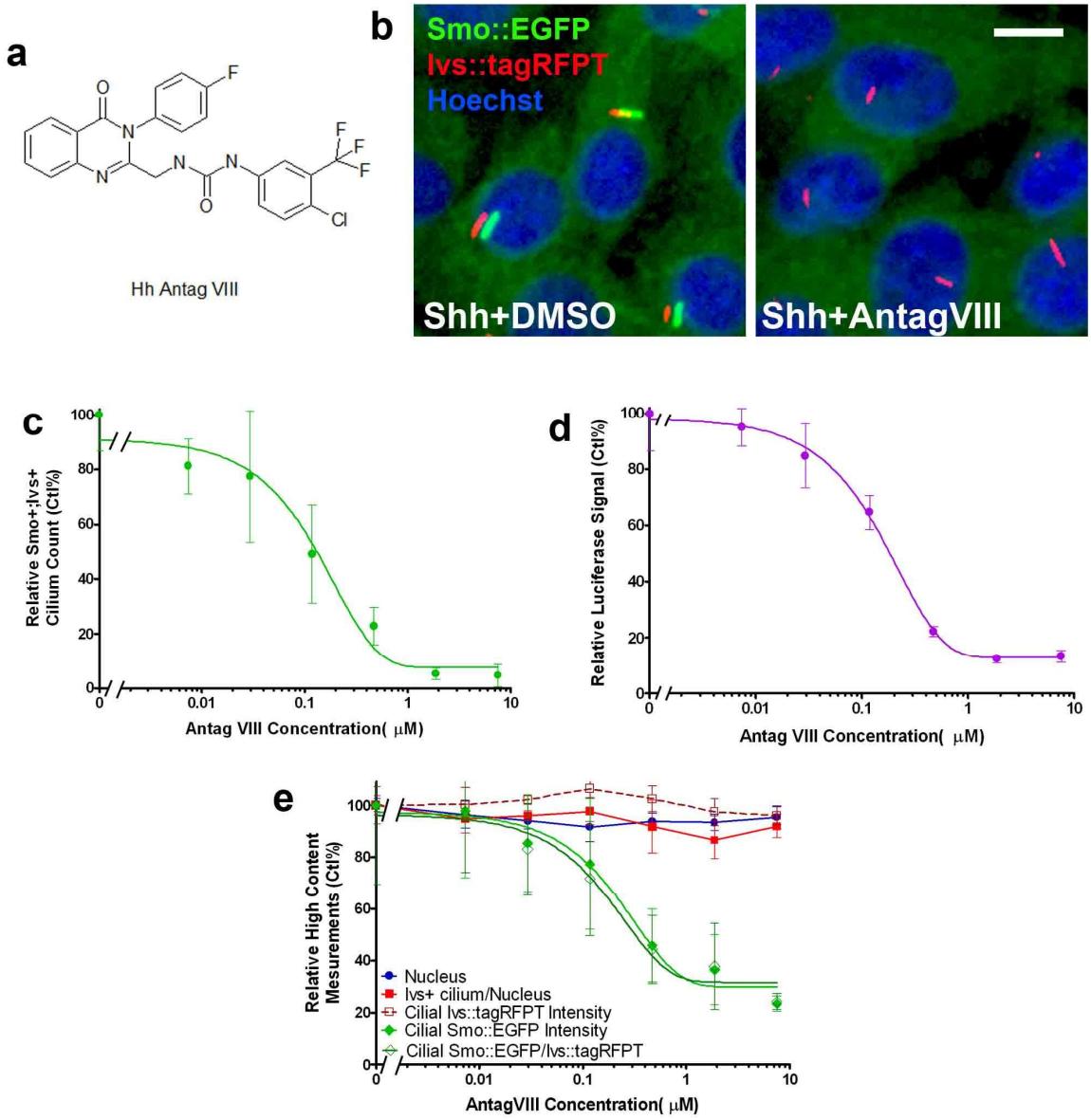

Supplementary Fig.5

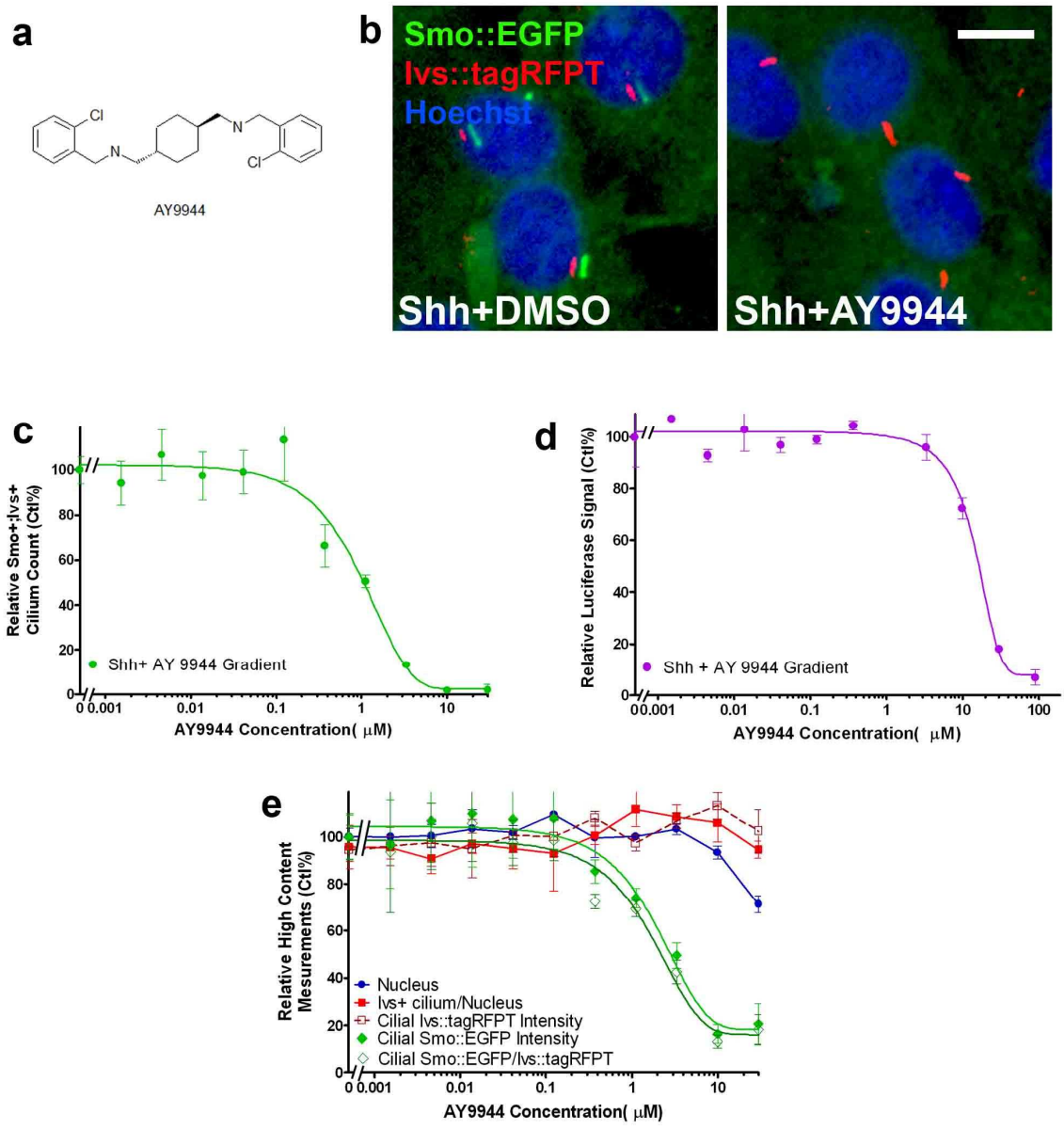

Supplementary Fig.6

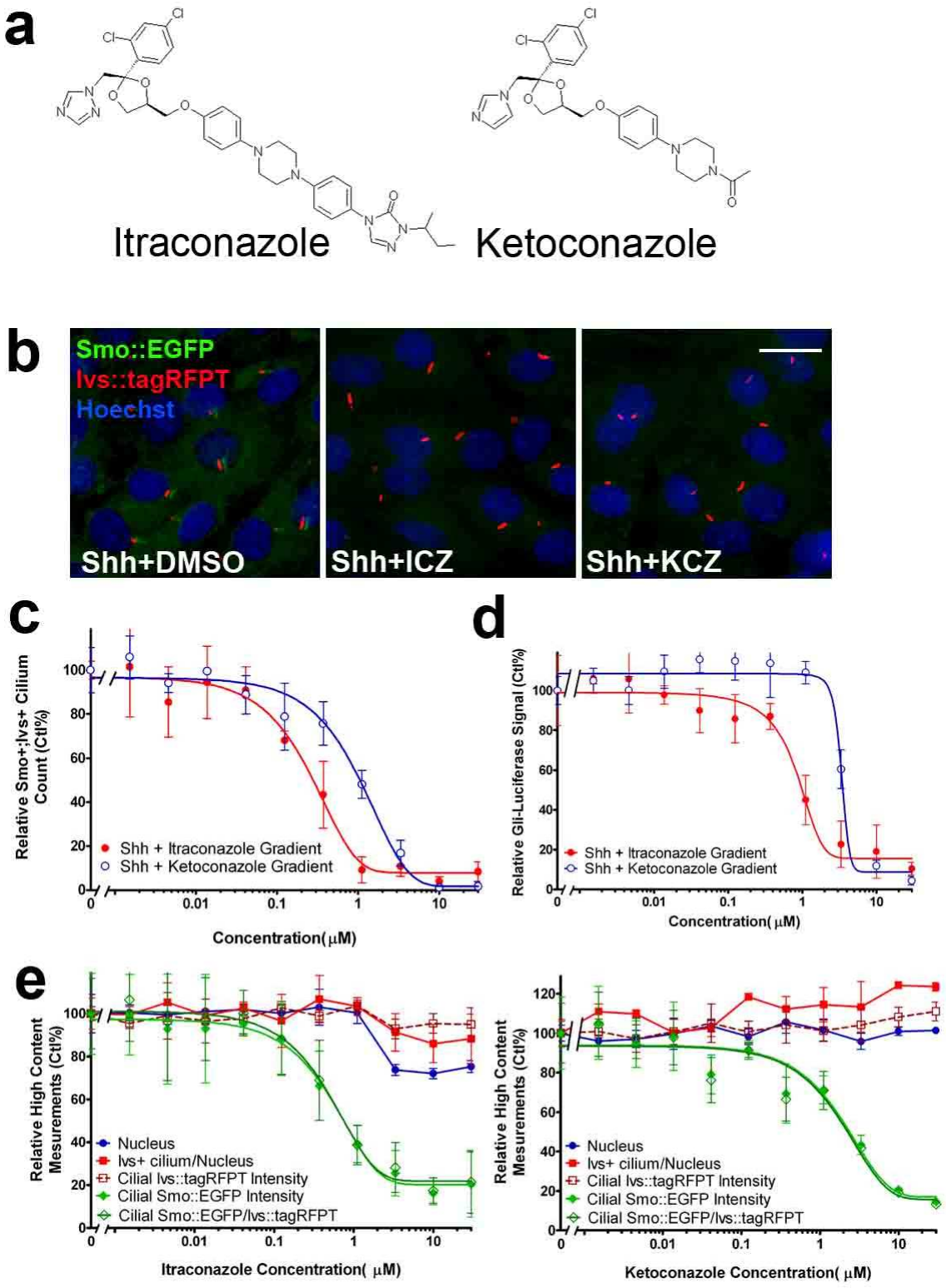

Supplementary Fig.7

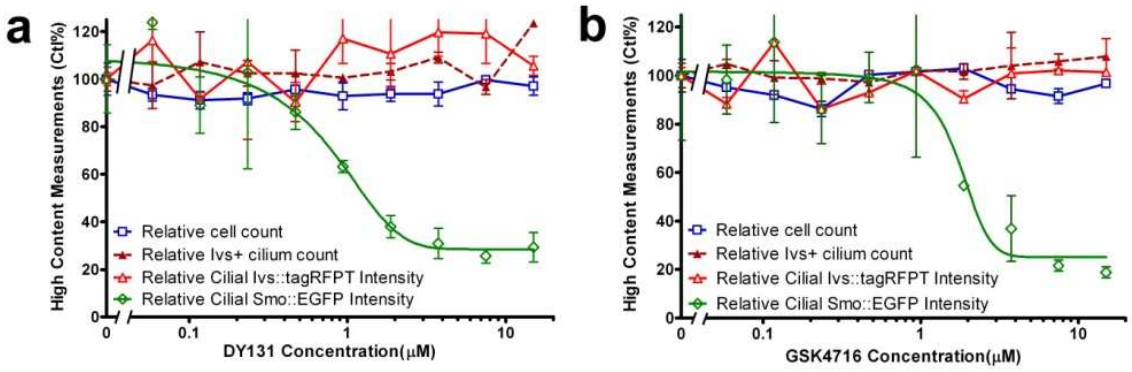

Supplementary Fig.8

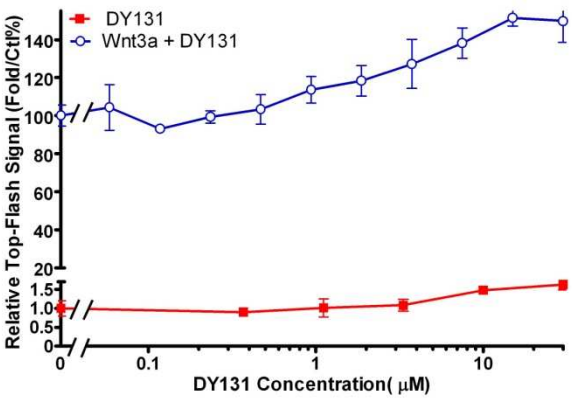

Supplementary Fig.9

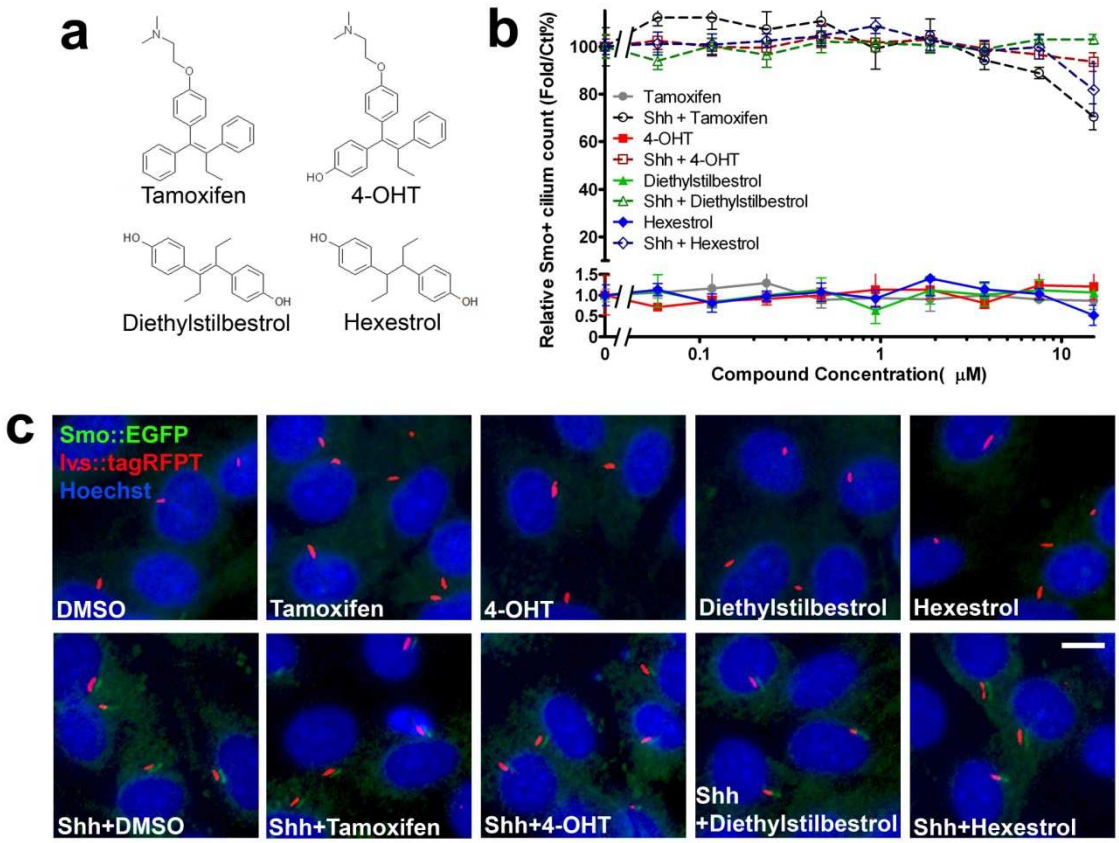

Supplementary Fig.10

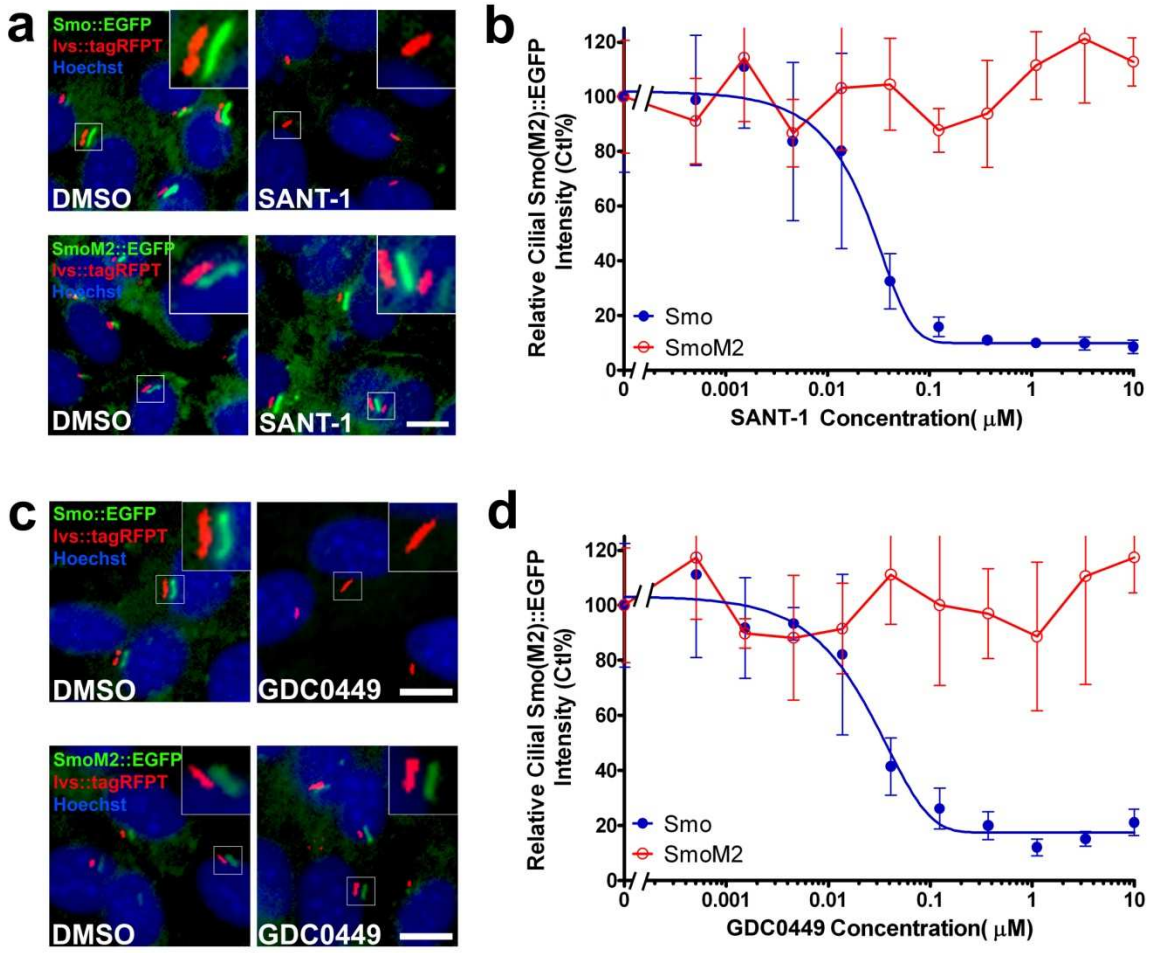

Supplementary Fig.11

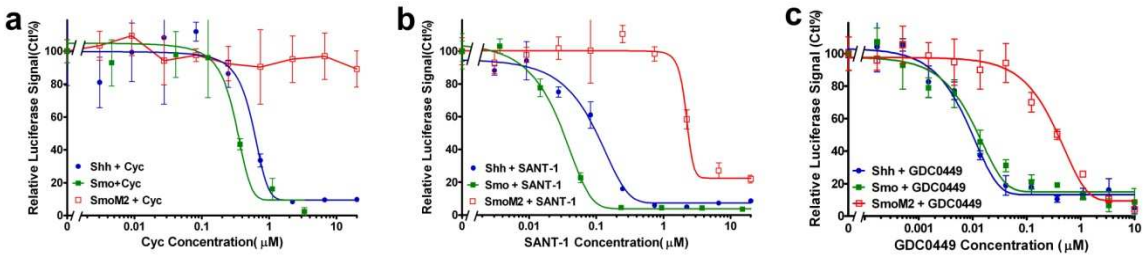

Supplementary Fig.12

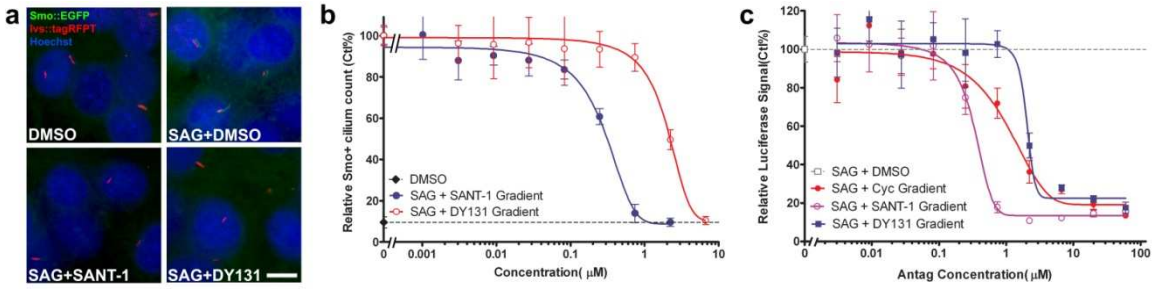

Supplementary Fig.13

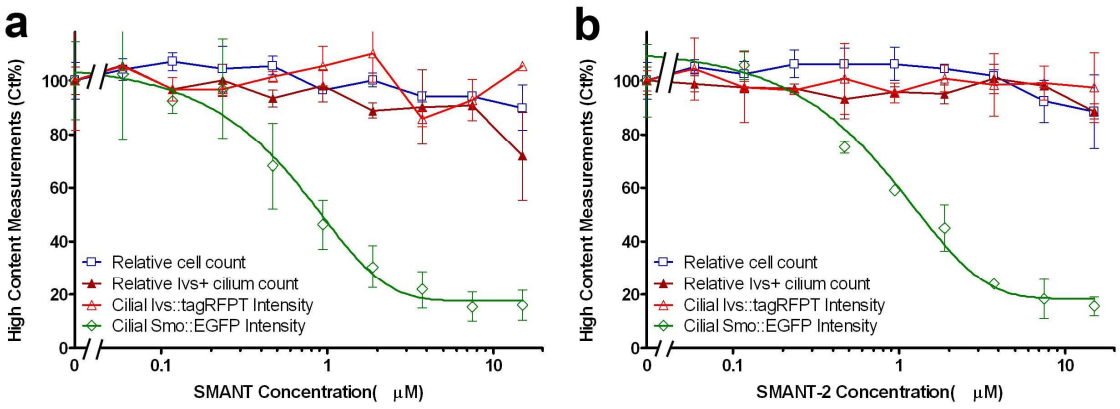

Supplementary Fig.14

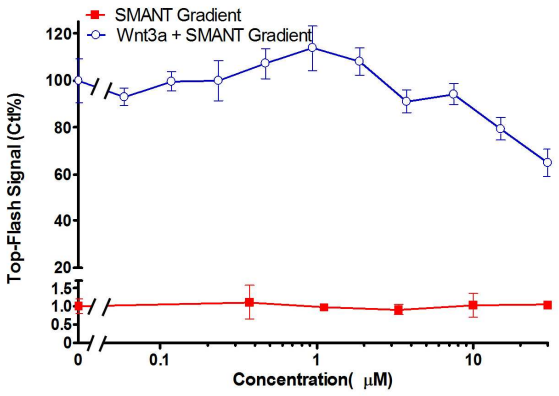

Supplementary Fig.15

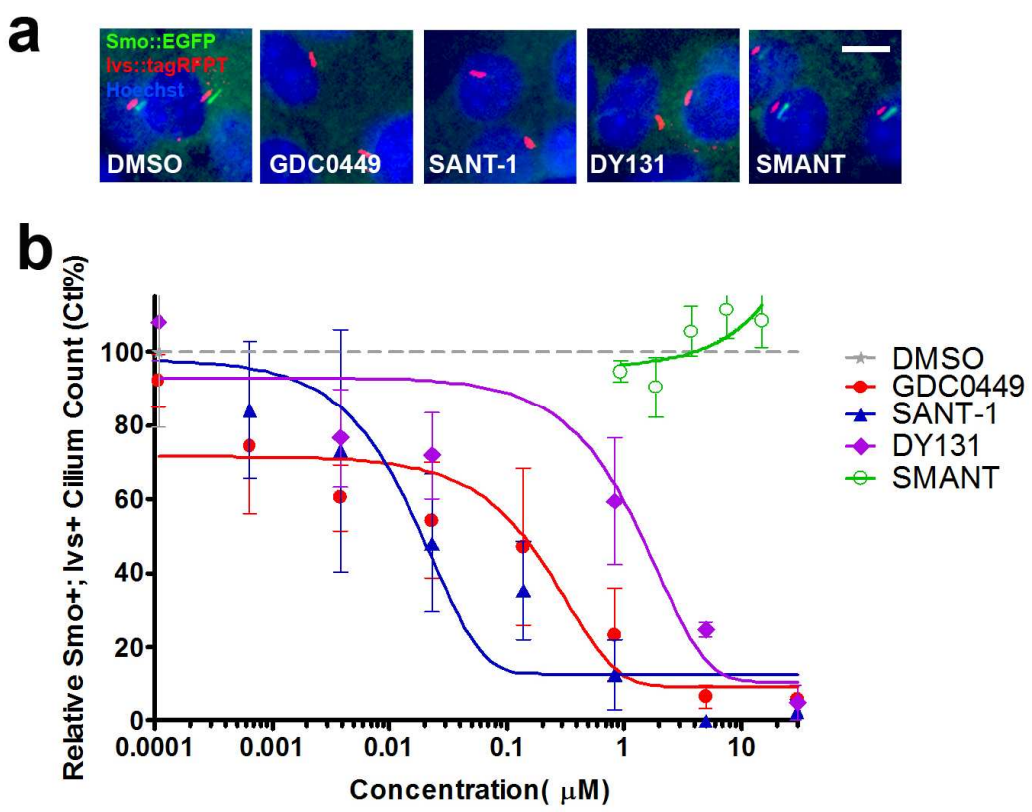

SupplementaryFig.16

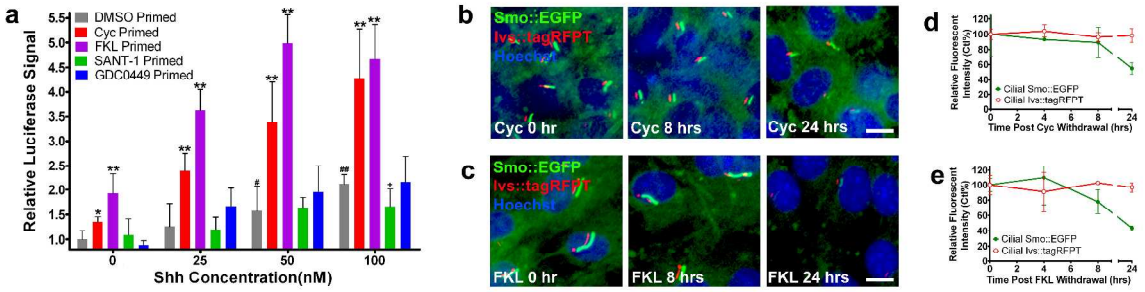

Supplementary Fig.17

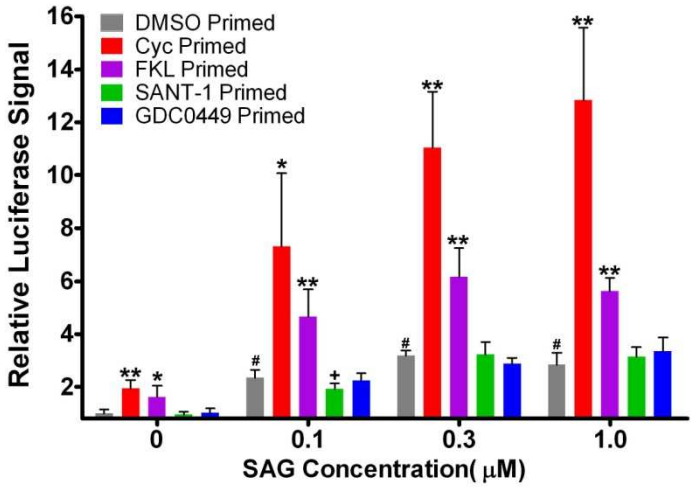

Supplementary Fig.18